

## Coherent Coatings of Refractory Metals

A general process for the electrodeposition of coherent coatings of the refractory metals.

S. Senderoff and G. W. Mellors

A series of publications (1) during the last 2 years have described the successful solution of a problem in electrochemistry that was first attacked by Michael Faraday. The papers discuss a newly discovered general process for the electrodeposition of coherent deposits of zirconium, hafnium, vanadium, niobium, tantalum, chromium, molybdenum, and tungsten.

Of these metals, only chromium can be electrodeposited from aqueous solutions—a successful industrial operation for over 30 years. Reports of processes, successful in the laboratory, for the electrodeposition of coherent deposits of molybdenum (2) and tungsten (3) by electrolysis of molten salts appeared about a decade ago, but these were highly specific to these metals. The molybdenum deposition was accomplished from a molten chloride solution and no other metal was found applicable; the tungsten deposition was effected from a molten borate-tungstate solution, and with modifications, the method has been extended only recently to molybdenum deposition (4). The new general process, applicable to eight of the nine metals of groups IVB, VB, and VIB (only titanium is excluded), effects coherent deposits by electrolysis of molten fluoride solutions.

Molten salts have been electrolyzed for many years for the purpose of depositing metals, but almost always

the metal (such as aluminum, magnesium, or sodium) is deposited in the liquid state, is immiscible with the electrolyte, and is separated by tapping, siphoning, or pouring to form a comparatively pure solid ingot. The refractory metals, however, have melting points that are too high (1855°C for zirconium to 3410°C for tungsten) to operate an electrolytic deposition process in the liquid state, and practical problems with materials for containers, electrodes, insulators, heaters, and so on have proved insurmountable. The metals are easily deposited in the solid state by electrolysis of molten salts, but not as coherent deposits; rather they are deposited as dendrites or powders, and recovered as mixtures with the solidified electrolyte (Fig. 1).

The cost of and difficulties involved in separating the metal from these mixtures, and in finally consolidating the metal by melting or sintering procedures to a solid object, have prevented any of these processes [with the exception of the Balke (5) process for preparation of tantalum] from attaining commercial importance. By the new process, however, which yields coherent deposits, one can not only prepare solid sheets suitable for direct mechanical processing, but also produce electroplated coatings and electroformed (6) objects of complex shape. The exceptional mechanical properties

at high temperatures of all the refractory metals, the excellent corrosion resistance of most of them, and the nuclear properties of some make them particularly interesting as coatings and electroforms.

We shall now describe what the new process does, how it operates, how it differs from previous related processes, and, finally, some experiments that give clues as to why it produces deposits that are coherent.

The product of the electrolysis is a dense, coherent sheet of metal; in Fig. 2 is a 60 by 50 centimeter sheet of niobium, approximately 1 centimeter thick, prepared by plating 0.5 centimeter of niobium on both sides of a niobium starting sheet that was approximately 0.3 millimeter thick. Figure 3 shows steel valves electroplated with tantalum (a) and an electroformed tungsten helix (b); the deposits have densities equal to the x-ray density of the bulk metal and are so pore-free that a coating of tantalum 0.1 millimeter thick protects the steel substrate of the valve in an environment of hot 20-percent HCl. The electroformed tungsten helix was made by plating on copper tubing and by removing the copper with nitric acid. The average wall thickness of the helix is approximately 0.6 millimeter. One can see that the surfaces of the plates in Fig. 3 (which are shown in the as-plated condition) are surprisingly smooth for the thicknesses involved. Chemical analyses of some of the metals produced by the process are reported in Table 1; purity usually exceeds 99.98 percent.

The metallographic structure of a niobium plate on copper is shown in Fig. 4. The columnar structure normal to the substrate and freedom from inclusions, precipitates, or voids are evident. Union Carbide Corporation has now undertaken commercial development of the process for the electrodeposition of four of the metals: niobium, tantalum, molybdenum, and tungsten.

Messrs. Senderoff and Mellors are on the staff of the Parma Research Laboratory of the development department of Union Carbide Corporation, Parma, Ohio.

## Operation

While the conditions for electrodeposition of coherent coatings vary from metal to metal, they are sufficiently similar that description of the process for depositing niobium can serve to illustrate the salient features of all. The electrolyte is prepared by dissolving about 16 percent (by weight) of potassium fluoniobate ( $K_2NbF_7$ ) in a eutectic mixture of alkali fluorides. The ternary eutectic KF-LiF-NaF and the binary eutectics KF-NaF and KF-LiF have been used. The solution is held under an argon atmosphere in a sealed cell (Fig. 5) and electrolyzed at a cathode-current density of 5 to 125 milliamperes per square centimeter, with niobium sheet or roundels used as anodes; the applied voltage is between 0.1 and 0.25 volt. In the case of niobium, the cell must be preelectrolyzed until the valence of the niobium is reduced to 4.0 to 4.2 to effect satisfactory operation; as the valence of the niobium increases, the current efficiency decreases from 100 percent at a valence of 4.1 to zero at a valence of 4.6.

Within rather broad limits, the composition of the electrolyte is not critical. For example, with a concentration of 5 percent (by weight) niobium fluoride in the ternary eutectic, the lower temperature of operation is around 700°C and the limiting current density is about 20 milliamperes per square centimeter; while at 30 percent the necessary operating temperature is nearer 825°C, above which the coherence of the plate suffers. At the upper temperature, moreover, volatility of higher-valent species may become troublesome in some systems. The use of KF-NaF eutectic requires a higher operating temperature than the ternary eutectic, with the same refractory-metal ion concentration, because of the higher liquidus temperature of the solution.

In general, therefore, the temperature range is established on the low end by the liquidus temperature of the electrolyte, and on the high end by the gradual loss of coherence of the deposit once a critical temperature is exceeded. This latter effect probably results from excessive dissociation of the fluoro complexes at the high temperatures.

The current-density range is established on the low side by the amount of noble impurities in the solution: the higher the amount, the higher the current density must be to minimize con-

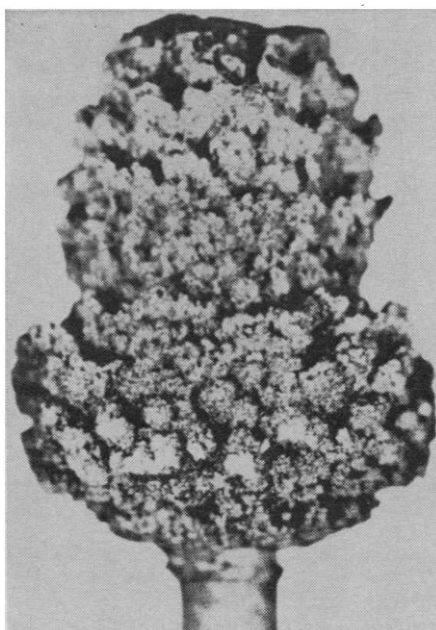


Fig. 1. Electrodeposit of zirconium from mixed chloride-fluoride system.

tamination of the deposit. The upper current-density limit increases with temperature and niobium concentration until the diffusion-limited current is reached; above this value alkali metal is deposited with disastrous results.

For successful operation the atmosphere over the solution must be essentially free of air and moisture. Noble metal impurities contaminate the deposits and sometimes adversely affect the coherence of the plates. Oxy salts and anions, such as hydroxide, oxide, and chloride, have been found undesirable in varying degrees. It is in use of the essentially pure fluorides without admixture of oxides, chlorides, and so on that this process differs from most of its predecessors that did not yield coherent deposits.

The effect of contamination of the

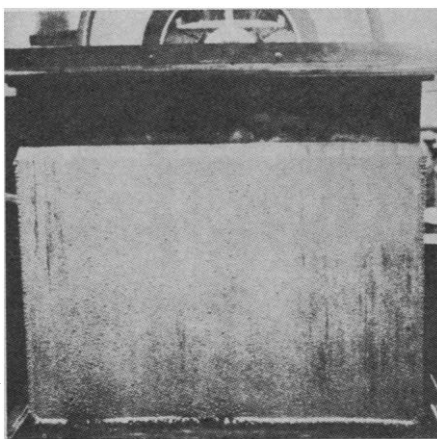


Fig. 2. Niobium sheet produced by electrorefining process.

electrolyte by moisture or oxygen is shown in Fig. 6: photomicrographs of the surface and the cross section of a deposit from this solution. The structure is clearly that of a compacted powder and, as shown in Fig. 6b, this noncoherent structure continues down to the substrate. However, since the coarseness of the structure increases with thickness, had the plating been stopped after only about 25 microns had been deposited, this poor structure may not have been evident. This point emphasizes the dangers of drawing structural conclusions from the observation of thin plates—a common practice in the earlier literature. We may add that even the thick (1 mm) deposit shown in Fig. 6 appeared superficially satisfactory to the naked eye and showed only severe brittleness as an effect of this poor structure; it would of course have been useless as a corrosion-resistant coating.

If the mean valence of the metal in solution is too high, the current efficiency of the process is reduced. Each of the metals is deposited at 100-percent cathode-current efficiency when it is present in solution in the appropriate valence state; that is, +5 for tantalum, +4.5 for tungsten, +4 for niobium, zirconium, and hafnium, and +3 for molybdenum, chromium, and vanadium. Higher valence values may result not only in reduced efficiencies, but also in poorer-quality plates. Control of the valence is not excessively difficult, and plating cells with an electrolyte charge of up to 1500 kilograms are being run commercially with success.

This process differs from its predecessors in that the electrodeposition by it is truly a Faradaic process; that is, Faraday's law is obeyed in that an equivalent weight of metal is deposited with the passage of 1 faraday of charge. The rate of deposition is measured by the current flowing and is independent of substrate, time of deposition, thickness of deposit, or other extraneous factors.

Delimarskii (7) and Smirnov (8) have stated that a coherent electrodeposit from molten salts can only be a diffusion alloy with the material of the substrate, and that if a pure metal is deposited it will be in powder or dendritic form. With the exception of the processes cited (2-4), all previous reports of coherent deposits have undoubtedly described production of diffusion alloys. While the statements of Delimarskii and Smirnov were, with

possibly only two exceptions, true at the time of their enunciation, our work indicates that they were generalizations. Much of the confusion in the literature stems from failure to distinguish between diffusion alloys and true electroplates; for instance, a commonly held belief propounded by Kroll (9) more than 25 years ago was that a solution that normally produced dendritic deposits at moderate current density would, at low current density, produce coherent plates. The fact is that even at low current density, if one waits long enough for the concentration gradient in the diffusion alloy to decrease with its increasing thickness, dendrites finally begin to form. At moderate current densities one almost always observes a thin diffusion layer below the dendritic deposit, and reducing the current density merely increases the time before the deposition of dendrites begins.

While diffusion alloys with the substrate are frequently valuable as corrosion-resistant or hard-facing coatings, they differ from true electroplated coatings in the following ways:

1) The composition of the diffusion alloy varies through the thickness of the coating; that of the electroplated coating is constant.

2) The rate of deposition of the diffusion alloy is determined by and is limited by the diffusion rates of the metals in the solid substrate. Since the compositions of the two ends of the diffusion couple are constant, the concentration gradient (and thus the driving force) must decrease with increasing thickness of the diffusion layer and result in an ever-decreasing and ultimately vanishing rate. The rate of deposition of the true electroplated coating is determined by the current, is limited by the diffusion rate of ions in the liquid electrolyte, and is independent of the substrate or rates of solid-state diffusion. While there is in principle no thickness limitation, slowly increasing roughness, with increasing thickness, imposes a practical limit.

3) The rate of deposition of a diffusion alloy decreases with increasing thickness, and falls to zero when the concentration of substrate metal in the surface of the alloy becomes too low. The function of the current is merely to maintain some metal or metal salt at the surface of the substrate to maximize the concentration gradient driving the diffusion process. Excess material that does not diffuse into the substrate may redissolve in the electrolyte or may

Table 1. Impurities in electroplated metals produced by the fluoride process. n.a., Not analyzed.

| Metal      | Impurity (ppm) |      |      |    |     |     |      |      |
|------------|----------------|------|------|----|-----|-----|------|------|
|            | O              | H    | N    | C  | Fe  | Ni  | Cr   | Cu   |
| Tantalum   | 27             | 6    | 4    | 4  | <11 | <7  | <11  | n.a. |
| Niobium    | 64             | 4    | <1   | 5  | 18  | <1  | 4    | 3    |
| Molybdenum | 11             | n.a. | n.a. | 14 | 20  | 100 | n.a. | n.a. |
| Tungsten   | 14             | 1    | <1   | 4  | 11  | 6   | 3    | 150  |

be deposited in the form of a poorly attached dendritic deposit overlying the diffusion layer.

These characteristics of the diffusion-alloy coatings prepared by electrolysis of molten salts have been confirmed by a number of workers. Sibert *et al.* (10) found that the titanium deposit produced by electrolysis of a mixed fluoride-chloride solution consisted of four layers: an alloy high in iron near the substrate, then a thin Fe-Ti intermetallic compound, next a  $\beta$ -Ti alloy high in iron, and finally, as the outer one-third of the deposit, a titanium-rich  $\alpha$ -Ti phase. This deposit could be built up to a maximum thickness of 25 to 50 microns, at which point dendrites began to be deposited. Stetson (11) stated that a titanium coating 0.25 millimeter thick, deposited from a molten fluoride system, had an average titanium content of 92 percent, while the outer surface reached a titanium content of 99 percent. The plating rate fell from 50 microns per hour initially to only 1.3 microns per hour when the plate thickness approached 0.8 millimeter. This may be considered a vanishingly small rate and corresponds to the thickness limit for the process. Stetson also found that metals that interdiffuse slowly with titanium are poor substrates for the process, thus confirming the dependence on substrate. Cook (12) produced beryllide coatings by means of the galvanic current produced between beryllium and

a substrate material immersed in molten fluorides; he found that he could increase the rate of deposition by supplementing the galvanic current with one produced by an externally applied potential until the total current corresponded to the diffusion rate of beryllium in the substrate at that temperature; increase in current beyond that value resulted in the deposition of dendrites; the thickness limit in this instance was 25 to 125 microns. Afino-genov *et al.* (8) concluded that coherent coatings can be electrodeposited from molten salts only as diffusion alloys, on the basis of an exhaustive metallographic study of the deposition of beryllium on copper, and the correlation of electrochemical and process variables with the composition of the alloy phases of the deposits.

The general process for depositing coherent coatings of the refractory metals that we have described can be shown in many ways to produce true electroplates; thus it is not subject to the limitations of the processes that produce diffusion alloys. The analyses of deposits (Table 1) were performed on the entire deposit from which the substrate had been removed by chemical or mechanical means. The fact that the coating was always better than 99.98-percent pure refractory metal demonstrates the absence of alloy formation. Inspection of the interface between the niobium and the copper (Fig. 4) shows sharp demarcation, with-

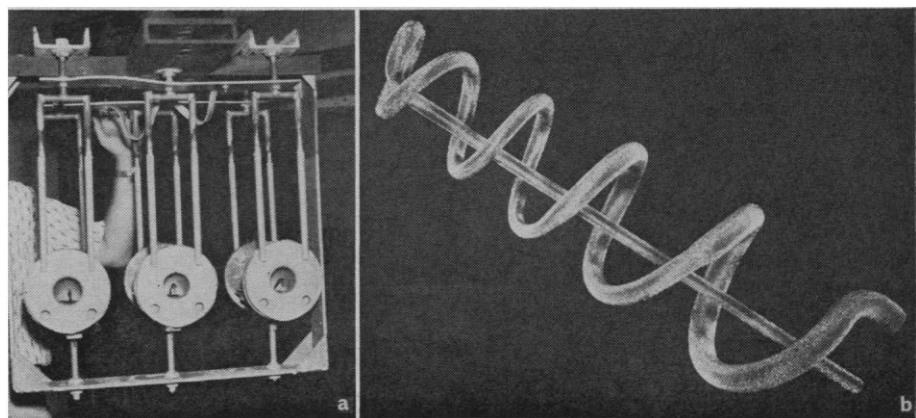


Fig. 3. a, Steel valves electroplated with tantalum. b, Electroformed tungsten helix.

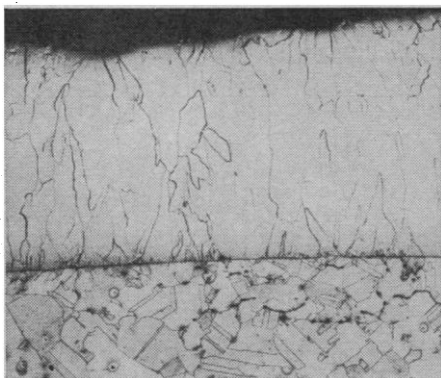


Fig. 4. Cross section of niobium (top) electrodeposited on copper ( $\times 55$ ).

out alloy layers between the two metals, confirming the fact that these two metals do not form solid solutions or intermetallic compounds. When molybdenum is deposited on nickel, however, at least two alloy layers are observed at the interface, confirming the well-known existence of solid solutions and intermetallics in the phase diagram of these metals. However, since the alloy layers comprise less than one-tenth of the total deposit, it is clear that the alloying occurred much more slowly than the deposition, that the deposition was independent of the alloying, and that the alloying was a phenomenon that occurred deep below the surface at which pure metal was being deposited.

Other phenomena that demonstrate that this process does not depend on diffusion alloying are its constant deposition rates at constant current density, independent of total thickness; and the fact that its constant current efficiency approaches 100 percent, independent of current density within wide limits and independent of total thickness.

Finally, when alloys such as Zr-Al and Mo-W or compounds such as  $ZrB_2$  are produced by this process, they are produced by codeposition on arbitrary substrates such as copper or stainless steel; further, they are of constant composition through the thickness of the layer and have no thickness limit other than the practical one cited above. The major value of a true Faradaic deposition process, compared to one producing diffusion alloys, is the applicability of the former to electrorefining while still producing coherent material (Fig. 2), and to electro-winning of metal from ores, with the production of solid sheets. The great thickness and purity of the deposit are also of great value in many coating and electroforming applications.

## Electrode Thermodynamic

### Considerations

A most intriguing problem that emerges from this work concerns elucidation of the special properties of pure fluoride systems that permit deposition of coherent deposits of these metals. One may start with the results of infrared-reflectance spectroscopy studies made of some of these plating solutions. It has been shown (13) that in the case of the  $KF-LiF-K_2TaF_7$  system the only identifiable tantalum-containing species in the solution, in the ranges of concentration and temperature useful for plating, is the  $[TaF_7]^{-2}$  complex ion. Further, no discernible change in the adsorption frequencies for this ion was observed over a temperature range of  $680^\circ$  to  $800^\circ C$  and a concentration range of 2 to 9 mole percent  $TaF_5$ —results indicating very high stability for this complex ion. When NaF was substituted for KF, however, the  $[TaF_6]^-$  ion was observed in addition to the  $[TaF_7]^{-2}$ . The lower stability of  $[TaF_7]^{-2}$  in the absence of  $K^+$  in the solvent may be correlated with difficulties encountered in the plating process in the absence of KF in the formulation. These and other measurements confirm that the fluoro complexes are generally more stable than the other halo complexes.

One may postulate that there is an optimum range of thermodynamic stability of complexes for the deposition of coherent plates, such that stabilities below this level result in excessive ease of reduction, which favors the growth of dendrites; and stabilities above this level make reduction too difficult and cause the preferential reduction of alkali metals from the solvent, which reduction causes powders and slimes to deposit. In the absence of quantitative information, one may explain the special property of fluoride systems by postulating that fluoro complexes happen to be in the right range of stability, particularly in a solvent with the correct cation formulation. Unfortunately, a more satisfying and more quantitative explanation of this type awaits additional thermodynamic data in this area.

### Electrode Reaction Mechanisms

Study of the mechanism of the electrode reactions by the method of chronopotentiometry has led to some very interesting results that merit dis-

cussion in detail, both for the light they throw on the electrodeposition process and as demonstrations of the effectiveness of the study of voltammetric transients in electrochemistry. Firstly we shall describe chronopotentiometry so that the results will be better understood.

The chronopotentiometric (or "galvanostatic") method, which has been described in detail (14), is essentially a constant-current electrolysis at a current density exceeding the limiting current density for the reaction under study, so that the potential-time relation during the electrolysis is as shown in Fig. 7. The end of a plateau occurs when the concentration of the diffusing reactant at the electrode surface falls to zero, and a current density is chosen so that this occurs within between a few milliseconds as a minimum and about 1 second as a maximum. The lower limit is that in which the time to charge the double layer is a significant portion of the total time, and the upper limit is the time when convection at the electrode becomes a significant process in mass transfer. These time limits make an oscillo-

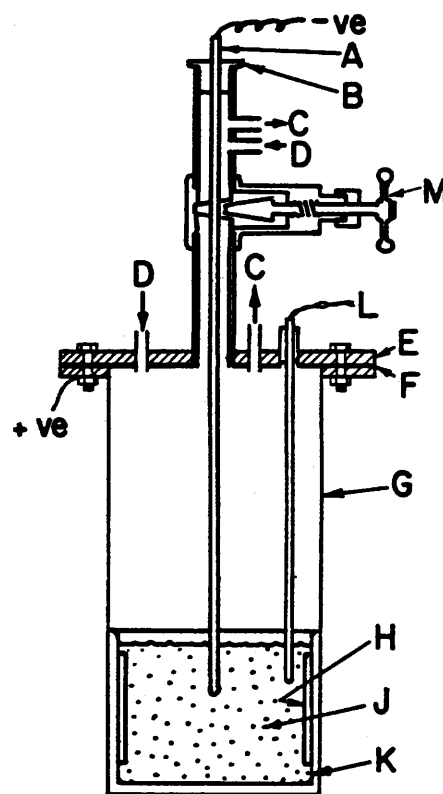


Fig. 5. Electroplating cell. A, Stainless steel cathode; B, Teflon stopper; C, argon outlets; D, argon inlets; E, steel lid; F, Teflon or Sauereisen gasket; G, Hastelloy-X can; H, niobium anode; J, fluoride melt; K, nickel crucible; L, thermocouple and well; M, gate valve (2.5 cm).

scope and camera the most convenient method for observing the potential-time relation.

A fundamental equation of chronopotentiometry applicable to diffusion-controlled systems is:

$$i\tau^{1/2}/C = \frac{1}{2}\pi^{1/2}FnD^{1/2} \quad (1)$$

where  $i$  is the current density (amp/cm<sup>2</sup>),  $\tau$  is the transition time (seconds) and equals the duration of a plateau in Fig. 7,  $C$  is the bulk concentration of the reacting species (moles/cm<sup>3</sup>),  $n$  is the number of electrons involved in the electrode reaction,  $D$  is the diffusion coefficient of the reacting species (cm<sup>2</sup>/sec), and  $F$  is the Faraday constant.

A fundamental equation for diffusion-controlled processes that are also thermodynamically reversible is:

$$E = E_1 + (RT/nF) \ln[(\tau^{1/2} - t^{1/2})/t^{1/2}] \quad (2)$$

where  $E$  is the potential (volts) at time  $t$  (seconds) on a plateau in the chronopotentiogram, and  $E_{1/4}$  is the potential at  $t = \tau/4$ .

The experimental parameters measured are  $\tau$  and  $E_1$ . Equation 2 is the Nernst equation with the usual concentration ratio in the logarithmic term replaced by time terms calculated from the time-dependence of the concentration during the chronopotentiometric run. The logarithmic term is analogous to the polarographic term  $(i_d - i)/i$ , and the  $E_1$  is analogous to the polarographic half-wave potential and bears the same relation to the thermodynamic standard electrode potential. The left side of Eq. 1 is called the transition time constant; its invariance with current density and concentration is an extremely sensitive and accurate criterion for diffusion control—for example, the absence of chemical kinetic factors from an electrochemical reaction. Moreover, the plot of  $E$  versus  $\log(\tau^{1/2} - t^{1/2})/t^{1/2}$  gives a straight line of slope  $2.3 RT/nF$  and provides a value for  $n$ , the number of electrons involved in the electrode reaction. With this value of  $n$ , one may calculate  $D$ , the diffusion coefficient of the reacting species, from Eq. 1.

Finally, in a reversible reaction  $E_1$  must be invariant with current density. Therefore, by running chronopotentiograms over a range of concentration and current density, one may establish unambiguously the reversibility of an electrode reaction, and the number of electrons involved in it by plotting  $\tan iT^{1/2}$  against  $C$ , noting its lin-

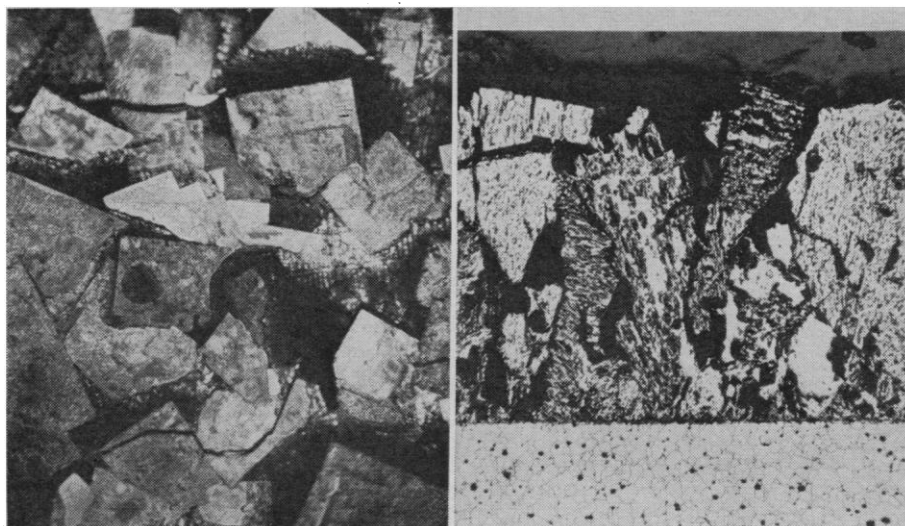


Fig. 6. Surface (left) and cross section of Nb compacted powder desposit ( $\times 40$ ).

earity and its extrapolation to zero at zero concentration, and plotting  $E$  versus the appropriate function of  $t$  and noting its linearity and slope. The behavior of  $E_1$  as current and concentration are varied is a further diagnostic criterion for the thermodynamic reversibility of the reaction.

When an electrode reaction occurs in a stepwise fashion (as in Fig. 7), each step may be treated in the same manner, its reversibility and  $n$  number may be established, and the  $E_1$  associated with each step may be determined. In addition, the  $n$  numbers of each step may be found by the relation

$$\tau_2/\tau_1 = (n_2^2/n_1^2) + 2(n_2/n_1) \quad (3)$$

a very sensitive indicator for the value of  $n$ .

Another direct check on reversibility can be obtained by reversing the current at or before the end of the plateau and by observing the nature of the reverse process: in a reversible system the  $E_1$  (forward) and  $E_1$  (backward) differ only by twice the  $IR$  drop of the system. Also, the value of the ratio  $t_b:t_f$  provides information on the solubility of the products of the electrode reaction.

Figure 7 is a chronopotentiogram obtained from a solution of  $K_2TaF_7$  dissolved in the NaF-KF-LiF eutectic mixture, which differs from the plating solutions for tantalum only in being more dilute in tantalum. The dilution is desirable experimentally in that moderate current densities (about 100 ma/cm<sup>2</sup>) may be used. The plateaus with  $E_1$ -values at  $-1.03$  and  $-1.26$  volts (15) represent two successive steps in the reduction of  $[TaF_7]^{-2}$ ,

in which the tantalum is pentavalent, to tantalum metal. The third step near  $-1.5$  volts represents the reduction of an aluminum impurity that arises from a porous alumina salt bridge used in the experiment, and that may be ignored. Figure 8 shows the plot of Eq. 1 for the first step of the reduction obtained from more than 80 chronopotentiograms over five-fold ranges of current density and concentrations. The linearity and extrapolation through the origin amply demonstrate the absence of chemical kinetic complications in this first step. The plot of Eq. 2 for the first reduction step is also accurately linear; it thus demonstrates Nernstian reversibility of this process. The value of  $n$  for the first step is found to be 3, and, since  $\tau_2/\tau_1 = 1.8$ , the value of  $n$  for the second step is 2, thus accounting for the five electrons required in the overall reduction of  $[TaF_7]^{-2}$  to tantalum metal.

Plots of Eqs. 1 and 2 for the second step of the reduction are widely variant from linearity, and the value of  $iT_2^{1/2}/C$  varies with concentration; one must conclude that the second step is irreversible and not diffusion-controlled. This conclusion is confirmed by cathodic-anodic chronopotentiometry, which shows great difference between the potentials of the cathodic and anodic processes.

Cathodic-anodic chronopotentiometry on the first step confirms its reversibility by showing nearly equal potentials for the forward and backward steps; it also indicates that the product of the first step is only very slightly soluble in the solution—deduced from the fact that the value of

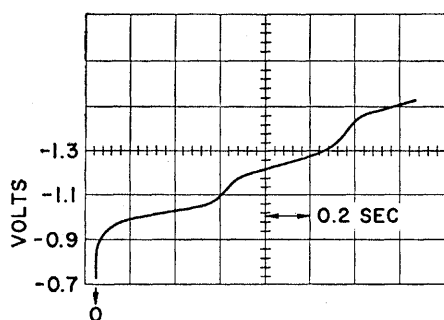
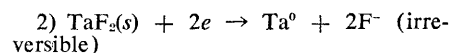
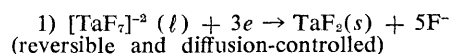


Fig. 7. Chronopotentiogram for reduction of tantalum in molten  $K_2TaF_7-NaF-KF-LiF$  solution.

$t_{anodic}/t_{cathodic}$  for the first step varies from 0.83 to 0.90, increasing with increasing current density. If the product were totally insoluble, this value would be 1.0; if completely soluble, 0.33 (14). The irreversibility of the second step may be caused by the insolubility of the intermediate and its probable presence in the solid state as a film on the cathode.

To summarize the results of this study, the mechanism for the reduction of the fluotantalate ion to tantalum metal occurs in two steps:

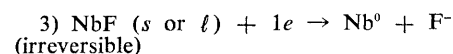
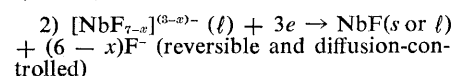
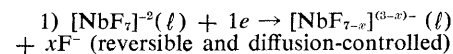


We may add that the diffusion coefficient and activation energy for diffusion of the reducible species of the first step,  $1.5 \times 10^{-5}$  square centimeters per second and 8.5 kilocalories per mole at  $750^\circ C$ , respectively, are of the expected magnitude for a highly coordinated ion such as  $[TaF_7]^{-2}$ .

A similar study of the niobium plating system gave somewhat similar results. In a solution with a mean valence of 4.0 to 4.2, there is a 3-electron reversible reduction at  $-0.756$  volt and a 1-electron irreversible reduction at  $-1.02$  volts (16). The material produced at  $-0.756$  volt is somewhat more soluble than the intermediate in tantalum plating, but it is still not completely soluble in the melt, as shown by a value of  $t_{anodic}/t_{cathodic}$  in cathodic-anodic chronopotentiometry of 0.54, compared to the 0.33 for a completely soluble product. The inability to plate niobium from solutions of mean valence approaching 5 arises from the rapid attack on this intermediate by the pentavalent solution, probably by the reaction  $3Nb^{5+} + Nb^{4+} \rightarrow 4Nb^{4+}$  (Fig. 9).

In Fig. 9a, at 30 milliamperes per square centimeter and a valence of

5, no reverse reaction at all is seen near the  $-0.756$ -volt reduction; the intermediate apparently is oxidized by the solution as fast as it is formed at this current density. At 100 milliamperes per square centimeter, one sees (Fig. 9b) a short reverse plateau indicating that at this current density its rate of formation was high enough for some to remain unattacked and to be oxidized on the reverse cycle. When the bath is electrolytically reduced to a mean valence for reduction of 4.34 (Fig. 9c), the attack on the intermediate is sufficiently slow that a reverse wave is seen, even at 30 milliamperes per square centimeter. If one plates at high-enough current density from a pentavalent solution, one does in fact obtain niobium metal, but only in dendritic form (17). It is therefore necessary to reduce the valence, and thus the rate of attack on the intermediate product of the electrode reaction, so that niobium may be deposited within the current-density range suitable for coherent deposition. To summarize the results with niobium deposition, starting from a solution of  $K_2NbF_7$  one observes three reduction steps:



In the usual tetravalent solution used for plating, only steps 2 and 3 are operative.

Chronopotentiometric measurements of the zirconium plating solution show a single 4-electron reduction step that appears to be irreversible; detailed interpretation of the results in this instance is more difficult than in the

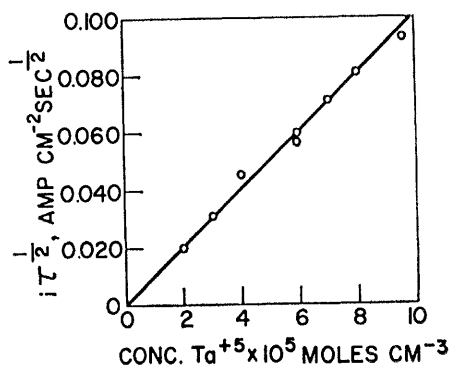


Fig. 8. Relation between transition time, current density, and concentration in chronopotentiometry of first step of tantalum reduction.

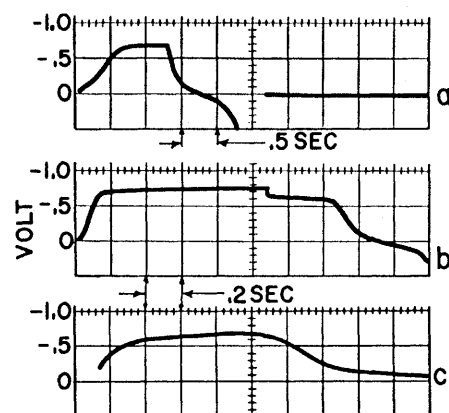


Fig. 9. Cathodic-anodic chronopotentiometry in niobium reduction. Current density ( $ma/cm^2$ ): 30 (a), 100 (b), 30 (c). Niobium valence: 5.0 (a), 5.0 (b), 4.34 (c).

others because the reduction wave is difficult to separate completely from a somewhat depolarized alkali-metal reduction wave. However, the source of irreversibility in this case may be the corrosion of the deposited zirconium by the electrolyte, with the liberation of potassium vapor; this has been observed macroscopically under certain conditions.

It may be significant that in all cases yet studied an irreversible step for the final deposition of metal accompanies coherent deposition. A brief examination of the chromium-deposition solution also shows a reversible reduction step followed by a highly polarized metal-production step; the source of this polarization is not yet understood. The only instance yet studied in which metal is produced in two completely reversible steps is that of iron where the  $Fe^{3+} \rightarrow Fe^{2+}$  and  $Fe^{2+} \rightarrow Fe^0$  steps satisfy exactly the criteria of chronopotentiometry discussed above. We have not been able, however, to deposit iron as coherent coatings—only as dendrites.

While it is still too early to state that an irreversible metal-producing step, one that involves some overvoltage at the electrode, is a necessary (though not sufficient) condition for the deposition of coherent deposits from molten salts, it is an eminently reasonable conclusion. In the normal process of growth, once a crystal is nucleated, one expects it to continue to grow to form a dendrite; interference with its growth by an insoluble film or corrosion of the tip of the developing dendrite by solvent should foster coherent plating as opposed to dendrite growth.

If this is the significant mechanism in the formation of coherent deposits,

the special properties of fluorides (compared to other halides) arise from the lower solubility or stability of lower fluorides in fluoride melts, compared to the analogous reduced compounds in the other halides. Considerable work on electrode-reaction mechanisms and on the chemistry of fluoride melts remains to be done before these tentative conclusions can be firmly substantiated.

### Summary

A general process has been developed for the electrodeposition of eight of the nine refractory metals of groups IVB, VB, and VIB as dense coherent deposits. It consists essentially of the electrolysis of a solution of the refractory metal fluoride in a molten alkali-fluoride eutectic mixture, and

has been shown to deposit a coating, unalloyed with the substrate, by a process that obeys Faraday's law. Some evidence exists that the electrode-reaction mechanism by which coherent coatings are deposited from molten salts incorporates an irreversible metal-producing step.

### References and Notes

1. G. W. Mellors and S. Senderoff, *J. Electrochem. Soc.* **112**, 266 (1965); **113**, 60 (1966); *Plating* **51**, 976 (1964); Canadian patent 688,546 (1964); S. Senderoff and G. W. Mellors, *J. Electrochem. Soc.* **112**, 841 (1965); **113**, 66 (1966).
2. S. Senderoff and A. Brenner, *J. Electrochem. Soc.* **101**, 16 (1954); U.S. patent 2,715,093 (1955); D. E. Couch and S. Senderoff, *Trans Metallurg. Soc. A.I.M.E.* **212**, 320 (1958).
3. G. L. Davies and C. H. R. Gentry, *Metalurgia* **53**, 3 (1956).
4. F. X. McCawley, C. B. Kenahan, D. Schlain, *U.S. Bur. Mines Rept. Invest.* **6455** (1964); D. Schlain, F. X. McCawley, C. Wyche, *J. Metals* **17**, 92 (abstr.) (1965).
5. C. W. Balke, U.S. patent 1,799,403 (1931).
6. An electroformed object is one produced by electroplating metal upon a substrate and by then removing the substrate so that the final

- object consists entirely of the electroplated metal.
7. Iu. K. Delimarskii and B. F. Markov, *The Electrochemistry of Fused Salts*, A. Peiperl and R. E. Wood, Transl. (Sigma, Washington, D.C., 1961), p. 270.
  8. A. I. Anfinogenov, M. V. Smirnov, N. G. Ilyushchenko, in *Electrochemistry of Molten and Solid Electrolytes*, M. V. Smirnov, Ed. Consultants' Bureau, New York, 1964), Engl. transl., vol. 2, pp. 35, 41.
  9. W. J. Kroll, *Trans. Electrochem. Soc.* **87**, 551 (1945).
  10. M. E. Sibert and M. A. Steinberg, *J. Electrochem. Soc.* **102**, 641 (1955).
  11. A. R. Stetson, *Mater. Design Eng.* **57**, 81 (March 1963); U.S. patent 3,024,174 (1962).
  12. N. C. Cook, U.S. patent 3,024,175 (1962).
  13. J. S. Fordyce and R. L. Baum, *J. Chem. Phys.* **44**, 1159 (1966).
  14. P. Delahay, *New Instrumental Methods in Electrochemistry* (Interscience, New York, 1954), chap. 8; W. H. Reinmuth, *Anal. Chem.* **32**, 1514 (1960).
  15. All potential values are with reference to the Ni/NiF<sub>2</sub> (1 mole percent) alkali fluoride reference electrode.
  16. Reduction of the pentavalent K<sub>2</sub>NbF<sub>7</sub>, the salt used in making up the solution, to the tetravalent state occurs reversibly at the rather noble E<sub>1/4</sub> value of -0.11 volt.
  17. R. E. Cumings and F. R. Cattoir, *U.S. Bur. Mines Rept. Invest.* **6506** (1964).
  18. Figures 1, 4, 5, and 7-9 were reproduced by permission of the *Journal of the Electrochemical Society*.

## Archeology and Its New Technology

Archeology comes of age with an interdisciplinary approach in expanding its research horizons.

Froelich Rainey and Elizabeth K. Ralph

In archeology, as in all branches of research, postwar technology has opened new horizons—not simply as a matter of increased efficiency, but as a remarkable acceleration in our acquisition of knowledge of man in his environments. Moreover, archeology is no longer limited to the “what” of prehistory, but is now making use of heretofore unsuspected methods of gleaning the “when,” the “how,” and, we hope, the “why” of man's prehistory. Perhaps of even greater importance, however, is the fact that some of those in the humanities, to their quiet surprise, find themselves working directly with physical scientists on specific research projects to solve technical problems of concern to both. In a small way, we are making the staggering crossover between the world of the

sciences and that of the humanities in a practical and, indeed, pleasant day-by-day experience. The physical scientist is being asked to provide a system of absolutes where few existed before, and the archeologist is learning that all chemists are not categorically alchemists. The happy result is that archeology has fallen heir to a number of these proliferating techniques and has acquired a new sophistication.

This article emphasizes those new techniques and the improvements in existing ones with which we have been working; in addition, a few pertinent although previously described techniques and developments at other institutions are outlined. Most of these techniques share a common ground in the application of some atomic or nuclear phenomenon: thermoluminescence dat-

ing is based on those electrons rendered metastable as a result of radiation damage; optical absorption magnetometers depend on the splitting of atomic energy levels; and a number of dating and analytical techniques rely on natural radioactive decay within the nucleus, or on transformations resulting from induced radioactive bombardment.

Of all the postwar developments, radiocarbon dating has had perhaps the most profound effect upon archeology. Literally thousands of radiocarbon dates obtained since the initiation of the method by Arnold and Libby (1) have aided in both the establishment and the revision of many archeological and geological chronologies. And the methods of detection of natural carbon-14 (primarily proportional gas counting techniques) are now sufficiently sensitive to permit investigation of some of those problems inherent in the radiocarbon dating method.

For normal dating calculations, the method assumes the constancy in past times of the atmospheric and oceanic inventories of carbon-14. But a fluctuation in the amount of carbon-14 in the atmosphere during a B.C. era was first suspected from the discrepancies found between radiocarbon dates and the es-

Dr. Rainey is professor of anthropology and director of the University Museum and of the Applied Science Center for Archaeology, University of Pennsylvania, Philadelphia. Miss Ralph, an associate in the department of physics at the University of Pennsylvania, is associate director of the Applied Science Center.